New insights into the analysis of the electrode kinetics of flavin adenine dinucleotide redox centre of glucose oxidase immobilized on carbon electrodes

Alexandr N. Simonov,[‡] Willo Grosse,[†] Elena A. Mashkina,[‡] Blair Bethwaite,[§] Jeff Tan,[††] David Abramson,[‡‡] Gordon G. Wallace,[†] Simon E. Moulton,[†,] Alan M. Bond[‡,*]*

[‡] School of Chemistry, Monash University, Clayton, Victoria, 3800, Australia

[†] ARC Centre of Excellence for Electromaterials Science, Intelligent Polymer Research Institute, University of Wollongong, New South Wales, 2522, Australia

[§] Monash eResearch Centre, Monash University, Clayton, Victoria, 3800, Australia

[††] IBM Research, Southgate, Victoria, 3006, Australia

[‡‡] University of Queensland, St Lucia, Queensland, 4072, Australia

ABSTRACT. New insights into electrochemical kinetics of flavin adenine dinucleotide (FAD) redox centre of glucose-oxidase (GlcOx) immobilized on reduced graphene oxide (rGO), single- and multi-walled carbon nanotubes (SW and MWCNT) and combinations of rGO and CNTs have been gained by application of Fourier Transformed AC voltammetry (FTACV) and simulations based on a range of models. A satisfactory level of agreement between experiment and theory, and hence establishment of the best model to describe the redox chemistry of FAD was achieved with the aid of automated *e*-science tools. Although still not perfect, use of Marcus theory with a very low reorganization energy (≤ 0.3 eV) best mimics the experimental FTACV data, which suggests that the process is gated as also deduced from analysis of FTACV data obtained at different frequencies. Failure of the simplest models to fully describe the electrode kinetics of the redox centre of GlcOx, including those based on the widely employed Laviron theory is demonstrated as is substantial kinetic heterogeneity of FAD species. Use of a SWCNT support amplifies the kinetic heterogeneity, while a combination of rGO and MWCNT provides a more favourable environment for fast communication between FAD and the electrode.

INTRODUCTION

Exploitation of the natural catalytic efficiency of redox enzymes, *via* incorporation into an electrical circuit, forms a basis for development of the next-generation of bio-devices. Sustainable evolution of this technology requires a thorough understanding of the enzyme electron transfer mechanisms. Electrochemical tools have proven to be extremely useful for this purpose.[1,2] In particular, voltammetric techniques applied to an enzyme immobilized on the surface of an electrode provide access to valuable mechanistic, kinetic and thermodynamic information. To date, classical DC cyclic voltammetric methods usually have been used for this purpose.[§] However, quantification of the enzyme electrode kinetics is often limited by poor faradaic-to-background current ratios typically encountered in protein film voltammetry. A complementary electrochemical method that provides substantial discrimination against background current is Fourier Transformed AC voltammetry (FTACV).[3] This method also provides a vast amount of data from a single experiment that facilitates more detailed quantification of the kinetics and thermodynamics. In particular, FTACV provides sensitivity with respect to discrimination of closely related mechanisms and facilitates detection of nonidealities of the enzyme/electrode interfaces.[4]

Glucose oxidase (hereinafter designated as GlcOx[**]) is an important and widely studied redox active enzyme, that has been used in the fabrication of glucose biosensors[5-7] and biofuel cells.[5,8] However, the vast majority of quantitative electrochemical studies of surface-confined GlcOx are

---

[§] Many important references up to 2008 can be found in the treatise by Leger and Bertrand.[2]

[**] The GlcOx acronym is preferred to GOD or GOx, widely used in the literature, to avoid confusion with acronym GO used for graphene oxide.

limited to estimation of the *apparent* heterogeneous electron transfer rate constant for reaction 1 (k^0_{2e}).

$$FAD^0 + 2e^- \underset{\longleftarrow}{\overset{k^0_{2e},E^0_{2e}}{\longrightarrow}} FAD^{2-} \quad (1)$$

where FAD is the flavin adenine dinucleotide cofactor of GlcOx.[9]

k^0_{2e} corresponds to the value of the rate constant at the reversible potential of reaction 1, which includes parameters of protonation of FAD^0 and FAD^{2-} (*vide infra*) and, therefore, is strongly dependent on the reaction conditions. Typically, k^0_{2e} has been evaluated on the basis of analysis of the peak-to-peak separations measured by DC cyclic voltammetry (ΔE_p) as a function of the scan rate (v) using classic Laviron theory based on Butler-Volmer kinetics with charge transfer coefficient, α, invariably assumed to be 0.50.[10] Reaction 1 reflects the model used in this form of data analysis.

With respect to use of DC cyclic voltammetry, Stevenson *et al.*[9] have confirmed that: (i) the majority of ΔE_p values used for calculation of k^0_{2e} for reaction 1 were governed in part by Ohmic (IR_u) drop rather than solely by kinetics due to problems with uncompensated resistance (R_u) encountered under typical experimental conditions; (ii) the dependence of ΔE_p on v for the $FAD^{0/2-}$ process does not fit in the classical theory[10,11] due to the presence of structural changes of the cofactor that accompanies electron transfer.[12] Differences in the protonation constants of oxidised and reduced forms of FAD,[12-14] electrode heterogeneity and other peculiarities are usually also ignored in quantification of electron transfer kinetics for the surface-confined $FAD^{0/2-}$ process.

In the present study, FTAC voltammetry has been introduced for analysis of the electrode kinetics of the redox centre of GlcOx in the expectation that new insights into the mechanistic details of redox transformations of the FAD cofactor will be gained. This method is far more sensitive to mechanistic nuances than the DC one. Eventually, it will emerge that no perfect model

is found for any of the scenarios evaluated, but FTACV method enables semi-quantitative comparison of the relative efficiency of the electron transfer between FAD and the support.

Basing on previous knowledge,[15] reduced graphene oxide (rGO), single- and multi-walled carbon nanotubes (SWCNT and MWCNT, respectively) as well as combinations of rGO and CNTs supports were used to achieve fast electron transfer between FAD and the electrode. These carbon materials are widely used for development of glucose sensors and anodes in biofuel cells (see, for example, references[9,15] and citations therein), although ambiguity in retention of the catalytic property of the enzyme after immobilization and the nature of interaction between GlcOx and carbon supports remains.[9,16] However the present study is exclusively focused on the electrode kinetics and mechanistic details of the surface-confined $FAD^{0/2-}$ process, while the bioelectrocatalytic properties of the similar GlcOx-based electrodes are discussed elsewhere.[15] The conclusions of the present study apply to the $FAD^{0/2-}$ process irrespective of whether FAD is allocated to the enzyme, disproportionated from the enzyme or present as a mixture of both scenarios.

EXPERIMENTAL

Materials. High-purity water (18 MΩ·cm; Millipore, USA) was used for preparation of all solutions. MWCNT (NanoAmor; 99.9 wt. % purity), SWCNT (Carbon Nanotechnologies Inc.; 85 wt. % purity), poly(ethyleneimine) (PEI; SigmaAldrich; 50 vol. % in H_2O), KH_2PO_4 (SigmaAldrich; ≥ 99 wt.%), K_2HPO_4 (SigmaAldrich; ≥ 99 wt.%), hydrazine (Sigma-Aldrich; 35 wt.% in water) and ammonia solution (Crown Scientific; 28 wt. % in water) were used as received from the manufacturer. Graphene Oxide (GO) was synthesized from graphite by a modified Hummers method.[17,18] Chemical reduction of GO to produce rGO was performed as

described elsewhere.[15] GlcOx from *Asperilligus niger* was purchased from Sigma-Aldrich, purified as described previously[19] and stored at -80°C in small aliquots (1.5 mL) at a concentration of 0.5 mg mL^{-1} in a 0.05 M phosphate buffer solution at pH = 5. The specific activity of the purified GlcOx was determined to be ~ 450 U/mg using an ABTS Assay.[20] High-purity nitrogen (99.999 %) was used to remove oxygen from all solutions used in electrochemical experiments.

Electrochemical instrumentation and procedures. Glassy Carbon (GC) electrodes (BAS; 3 mm diameter) were polished using aqueous Al_2O_3 (1, 0.3, 0.1 and 0.05 μm) slurries, sonicated in water for 10 min, dried under a N_2 stream and used as substrates for deposition of dispersions of carbon materials and GlcOx.

Individual aqueous suspensions of rGO, MWCNTs, SWCNTs as well as combined suspensions containing rGO (91 wt.%) + MWCNT (9 wt.%) or rGO (91 wt.%) + SWCNT (9 wt.%) were prepared as described elsewhere[15] using horn sonication (Branson Digital Sonifier – 500W) in an ice bath to form stable composite dispersions (0.25 mg mL^{-1}). The carbon dispersions were characterized by scanning electron microscopy (SEM) using a JEOL cold field emission gun scanning electron microscope and with a Leica optical microscope. GlcOx solution (0.5 mg mL^{-1}) was mixed with the carbon material dispersions just prior to deposition.

Modified working electrodes were fabricated by pipetting 5 μL aliquots of the appropriate suspension on the surface of a GC electrode, which was then kept at 5°C until evaporation of water was complete. Next, a layer of PEI (5 μL of 1 mg mL^{-1} solution in 0.5 M NaCl) was applied to entrap the enzyme, and the electrode was again allowed to dry at 5˚C. The total amount of deposited carbon materials and GlcOx (for enzyme-containing electrodes) was 0.625 and 1.25 μg, respectively. Total surface area of the deposited carbon materials (see Table S1, Supporting

Information) was evaluated on the basis of the BET specific surface areas of carbon nanotubes and rGO provided by the manufacturer and reported in the literature,[21] respectively.

Voltammetric measurements were undertaken in a conventional three-electrode cell thermostated at 37°C using an eDAQ potentiostat (Echem software v2.0) or a custom-made FTACV instrument.[3] Ag|AgCl|3 M KCl and high surface area Pt wire were used as reference and auxiliary electrodes, respectively. Prior to undertaking experiments, 0.5 M K_2HPO_4 + KH_2PO_4 aqueous buffer as supporting electrolyte solution (pH 7.0) was deaerated by purging with N_2 for at least 20 min. During measurements, a N_2 atmosphere was maintained inside the cell.

Theory. Simulations of the DC and AC voltammograms are based on Butler-Volmer or Marcus formalisms for description of the heterogeneous electron transfer kinetics[4,22] and were undertaken using the Monash Electrochemistry Simulator (MECSim) software.[23]

To minimize undesirable 'ringing' effects that emerged during the Fourier Transform – band filtering - inverse Fourier Transform (FT/iFT) routine,[24] an *ad hoc* generated window function (see Fig. S1 and accompanying comments in Supporting Information) was applied in the band filtering stage of data processing. Theory-experiment comparisons were performed both heuristically and with the aid of the Nimrod/G tool,[25,26] which is the part of the Monash University *e*-science tool kit. This software allows sweep experiments to be performed where each parameter is assigned a set of values, and the result of the sweep determines the level of agreement between the simulation and experiment for each combination of the varied parameters. When using Nimrod/G data analysis, the quality of fit was quantified as relative root mean square deviation (ψ), which is the statistical measure of the relative differences between values predicted by a model and experimental data:

$$\psi = \sqrt{\frac{\sum_{i=1}^{N}(f^{exp}(x_i) - f^{sim}(x_i))^2}{\sum_{i=1}^{N} f^{exp}(x_i)^2}},$$

where $f^{exp}(x)$ and $f^{sim}(x)$ are experimental and simulated functions respectively and N is the number of data points.

RESULTS AND DISCUSSION

Electrode characterization. Previously developed strategies for fabrication of the GlcOx-modified carbon electrodes[15] using aqueous dispersions of the carbon supports and a PEI stabilizing layer for entrapping and preventing FAD loss during electrochemical measurements were adopted in the present study. As previously demonstrated,[15] rGO based aqueous dispersions exhibit reasonable stability and homogeneity owing to the hydrophilicity of carbon material, which is rich in oxygen-containing functional groups (see optical images taken from the rGO, rGO-SWCNT and rGO-MWCNT suspensions in Fig. S2, Supporting Information). As expected, aqueous suspensions of MWCNT and SWCNT, not subjected to preliminary hydrophilization procedures, tended to agglomerate in the absence of polymer dispersing agents or surfactants (Fig. S2d and e, Supporting Information). However, these reagents were avoided to maintain a GlcOx-friendly environment. SEM micrographs of the MWCNT and SWCNT layers deposited from the aqueous dispersions revealed entangled networks of nanotubes (Fig. S3, Supporting Information), so that deposition on the GC surface resulted in inhomogeneous layers.

Notwithstanding the lack of homogeneity of dispersions of carbon nanotubes, deposition of enzyme-free and GlcOx-containing MWCNT and SWCNT layers onto GC produced the expected background current associated with the double-layer capacitance and pseudocapacitance of the carbon surface under conditions of DC cyclic voltammetry (Fig. 1). Higher mass-weighted background current of the SWCNT electrode as compared to MWCNT is associated with

differences in specific areas (A_{BET}) of single- and multi-walled nanotubes (Table S1), although a direct proportionality between A_{BET} and measured currents is not found (Fig. 1). Presumably, variation in pseudocapacitance is due to difference in the population of defects and functional groups on the surface of SWCNT and MWCNT[27] (determined by the conditions of synthesis of the carbon materials provided by the manufacturers). A high population of functional groups on the rGO surface provides the highest pseudocapacitance, while substitution of 9 wt. % of the reduced graphene oxide by SWCNT or MWCNT decreases the background current (Fig. 1).

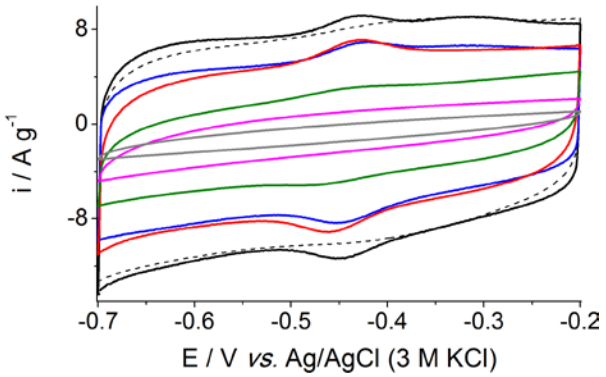

Figure 1. DC voltammetry (v = 0.050 V s^{-1}) for bare GC (*grey*), unmodified rGO (*black*, dashed) and GlcOx-modified rGO (*black, solid*), MWCNT-rGO (*blue*), SWCNT-rGO (*red*), SWCNT (*green*), MWCNT (*magenta*) electrodes in contact with 0.5 M K_2HPO_4 + KH_2PO_4 aqueous electrolyte solution (pH = 7.0). T = 310 K. Currents are normalized to the theoretically expected mass of the carbon materials.

In accordance with a previous report,[15] GC electrodes modified with GlcOx in the absence of supporting carbon materials as well as with a GlcOx containing suspension of MWCNTs did not exhibit notable $FAD^{0/2-}$ faradaic current in either DC (Fig. 1) or FTAC voltammograms (not shown). However, application of rGO, SWCNT and combinations of rGO with both single- and multi-walled CNTs as supports generated well-defined faradaic currents associated with redox

transformation of FAD (Fig. 1). Mid-point potentials, calculated as the average of the oxidation and reduction peak potentials in voltammograms for $FAD^{0/2+}$ process (E_m), fall within the range reported for surface-confined GlcOx and FAD in other studies (see[9] and refs. therein) and are slightly dependent on the nature of the carbon support (Table 1).

Table 1. Characteristics of the FAD-based electrodes. [a]

Support	Γ / pmol cm^{-2} [b]		DCV [c]		FTACV [d]				
	Expected	Detected	E_m / V	k^0_{2e} / s^{-1}	E^0 / V	Model and k^0_{app} / s^{-1} I	II	III	IV
SWCNT	3.6	0.6 ± 0.1	-0.450	2-3	-0.459	10-20	18-37	300-550	3-7
rGO	4.2	1.3 ± 0.5	-0.444	2-5	-0.454	60-110	90-120	1400-2000	16-21
MWCNT-rGO	4.5	1.4 ± 0.1	-0.437	2-5	-0.439	130-150	165-190	2200-3000	22-30
SWCNT-rGO	4.1	2.3 ± 0.2	-0.444	2-3	-0.450	20-40	40-50	600-700	6-10

[a] The data are derived from measurements on 3 electrodes of each configuration. The MWCNT support is not included as there was no observable faradaic current associated with FAD electrochemistry.

[b] Theoretically expected and experimentally detected surface concentrations of FAD normalized to the surface area of the carbon material(s) deposited on the electrode (Table S1).

[c] Mid-point potentials (*vs.* Ag/AgCl (3 M KCl)) and apparent k^0_{2e} values estimated from DC voltammetric data using classic theory[10] based on reaction 1.

[d] Parameters for FAD redox transformations determined by comparison of experimental data with simulations of FTAC voltammograms (f = 9 Hz, ΔE = 0.12 V). Models used in simulations are: **I**, **II** and **III** – two consecutive electron transfers (reactions 2, 3) with $k^0_{0/\bullet-} = k^0_{\bullet-/2-}$ and $E^0_{0/\bullet-} = E^0_{\bullet-/2-} = E^0$ (**I**, **II**) or $E^0_{\bullet-/2-} = E^0_{0/\bullet-} + 0.4$ V (**III**, $E^0 = E^0_{0/\bullet-} + 0.2$ V = $E^0_{\bullet-/2-} - 0.2$ V) using BV relationship (**I**, **III**) or Marcus theory with $\lambda = 0.2$ eV (**II**); **IV** – simultaneous two electron transfer (reaction 1) using Marcus theory with $\lambda = 0.2$ eV.

The surface concentration of the electrochemically active redox cofactor (Γ / pmol cm^{-2}, normalized to the surface area of the carbon material(s) shown in Table S1) was estimated from the charge calculated by integrating the oxidation component of stabilized DC voltammograms in the -0.50 – -0.35 V potential range, after correction to the background current. The latter was either obtained for the FAD-free electrode containing the same amount of the appropriate carbon material(s) or a linear approximation in cases when the FAD-containing and blank electrode data did not fully match. Generally, both background correction methods provided similar outcomes, although application of a linear background could result in slight overestimation of Γ. Juxtaposition of the expected values (taking into account the dimeric structure of GlcOx[28]) and experimentally detected Γ values (Table 1) reveals that the carbon materials differ in their abilities to immobilize FAD. The highest efficiency of immobilization of 55 % was achieved with the rGO-SWCNT composite carbon support.

Analysis of DC voltammetric data. The theory elaborated by Laviron[10] has been widely applied to DC voltammetric data derived from the surface-confined redox centre of GlcOx to calculate k^0_{2e}. However, in addition to the need to account for IR_u drop, not accommodated in this theory, there are other fundamental problems concerning the use of this treatment based on the assumption of the Butler-Volmer (BV) model with α = 0.50 and the simultaneous transfer of two electrons.

Under conditions commonly used for voltammetric studies of GlcOx (near neutral pH, moderate temperatures), FAD undergoes what often appears to be an essentially simultaneous two-electron transfer *via* reaction 1 accompanied by protonation processes. In reality, this process is more likely to involve consecutive one-electron transfers (reactions 2 and 3) where each participating species is capable of two consecutive protonation reactions. Thus, the full mechanism for FAD

electrochemical transformation could comprise 6 charge-transfer and 6 protonation stages. However, according to Smith and co-workers,[13,14] under most conditions, each oxidation level of the FAD cofactor is dominated by only one protonated form thereby allowing simplification of the redox scheme. Furthermore, the reaction scheme can be written as in charge-transfer reactions 2 and 3 assuming diffusion controlled (reversible) kinetics of protonation. Under this assumption, the protonation constants are introduced into the electrode kinetic formulation problem *via* use of a modified formal potential (E^0). In this scenario, E^0 for reaction 2 ($E^0{}_{0/\bullet-}$) can become more negative than that of reaction 3 ($E^0{}_{\bullet-/2-}$) giving rise to an apparently simultaneous two-electron transfer reaction.[12-14] For this reason, apparent k^0 values (designated $k^0{}_{app}$ in later discussion) are actually reported.

$$FAD^0 + e^- \underset{}{\overset{k^0_{0/\bullet-},E^0_{0/\bullet-}}{\rightleftharpoons}} FAD^{\bullet-} \qquad (2)$$

$$FAD^{\bullet-} + e^- \underset{}{\overset{k^0_{\bullet-/2-},E^0_{\bullet-/2-}}{\rightleftharpoons}} FAD^{2-} \qquad (3)$$

Peak-to-peak separations measured in DC voltammetry (ΔE_p) are a quantitative indicator of the facility of the electron transfer for both systems described either by reaction 1 or by reactions 2 and 3. However, there is no direct relationship between $k^0{}_{2e}$ of net reaction 1 and the *apparent* $k^0{}_{0/\bullet-}$ and $k^0{}_{\bullet-/2-}$ rate constants associated with reactions 2 and 3. Thus, while reaction 1 is amendable to analysis by classical theory,[10] straightforward calculation of k^0 and E^0 parameters for reactions 2 and 3 on the basis of ΔE_p values is not realistic. Simulations are in fact required to explore the nuances, and even these have been used with simplifying assumptions establishing the relationship between $k^0{}_{0/\bullet-}$ and $k^0{}_{\bullet-/2-}$ and between $E^0{}_{0/\bullet-}$ and $E^0{}_{\bullet-/2-}$. For example, Armstrong *et al.*[29] assumed equality of electron transfer rate constants and formal standard potentials for reactions 2 and 3 when undertaking theoretical analysis of the square-wave voltammetric responses from the surface-confined fumarate reductases containing redox active FAD sites.

Fig. 2 juxtaposes experimental DC voltammograms obtained for the GlcOx-modified MWCNT-rGO electrode with the theoretical curves simulated for reaction 1 or reactions 2 and 3 (assuming $k^0_{0/\bullet-} = k^0_{\bullet-/2-}$) using the BV formalism with $\alpha = 0.50$.

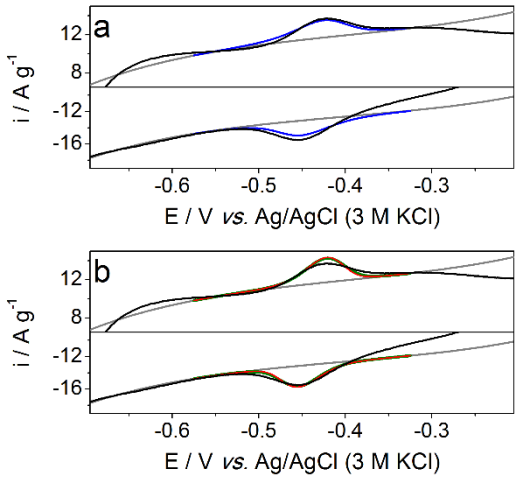

Figure 2. Comparison of experimental DC cyclic voltammogram ($v = 0.10$ V s^{-1}) obtained with the GlcOx-modified MWCNT-rGO electrode in contact with 0.5 M K_2HPO_4 + KH_2PO_4 aqueous electrolyte solution (pH = 7.0) (*black*) and voltammograms simulated for a surface-confined species ($\Gamma = 1.4$ pmol cm^{-2}) undergoing either two consecutive one-electron transfers with $k^0_{0/\bullet-} = k^0_{\bullet-/2-} = 12$ s^{-1}, $E^0_{0/\bullet-} = E^0_{\bullet-/2-} = -0.438$ V (*blue*) and $k^0_{0/\bullet-} = k^0_{\bullet-/2-} = 310$ s^{-1}, $E^0_{0/\bullet-} = -0.638$ V, $E^0_{\bullet-/2-} = -0.238$ V (*green*) or a simultaneous two-electron transfer ($k^0_{2e} = 4$ s^{-1}, $E^0_{2e} = -0.438$ V) (*red*). Note that the *green* and *red* curves are indiscernible. *Grey* curve represents the simulation of the background current. Other simulation parameters: Butler-Volmer model with all $\alpha = 0.50$; $A = 3.46$ cm^2, $R_u = 71$ Ω, $C_{DL} = 22.2$ μF cm^{-2}, T = 310 K. Simulated curves are shown in the region of occurrence of detectable faradaic currents only. Currents are normalized to the theoretical mass of carbon materials expected for the experimental data.

Domination of the background current hinders detailed comparisons of the experimental and simulated Faradaic current data. Nevertheless, some preliminary conjecture can be made on the basis of the results presented in Fig. 2. In particular, the simplest models assuming simultaneous two-electron transfer (reaction 1) or consecutive one-electron transfers *via* reactions 2 and 3 with $\Delta E^0 = E^0_{0/\bullet-} - E^0_{\bullet-/2-} = 0.4$ V are essentially the same and predict much sharper voltammetric processes than observed in the experiment. On the other hand, modelling based on reactions 2 and 3 with equal E^0 values more acceptably describes the shape of the experimental voltammogram (Fig. 2), although thermodynamic and/or kinetic heterogeneity almost certainly present in this case and commonly associated with surface-confined enzymes[2-4,29,30] or engagement of Marcus theory with low reorganization energies (λ) also could broaden the voltammetric shape.[30]

FTAC voltammetry at low frequency: heuristic comparisons of experimental and simulated data. FTACV provides a method for probing mechanistic nuances in considerably more detail than provided with DC cyclic voltammetry. Hence studies of the electrochemistry of FAD immobilized on different carbon supports were undertaken by examination of the first 10 AC harmonic components of the FTAC voltammograms derived from a single sine wave perturbation of frequency f and amplitude ΔE superimposed onto the DC potential ramp. A comparatively high value of $\Delta E = 0.12$ V was used to maximize the non-linearity and hence obtain enhanced higher order harmonics currents. Low-frequency (9 Hz) FTACV measurements provided up to 10 well-defined AC higher-order harmonic components associated with oxidation and reduction of surface-confined FAD, as exemplified in Figs. 3 and 4 for the GlcOx-modified MWCNT-rGO and SWCNT electrode configurations, respectively.

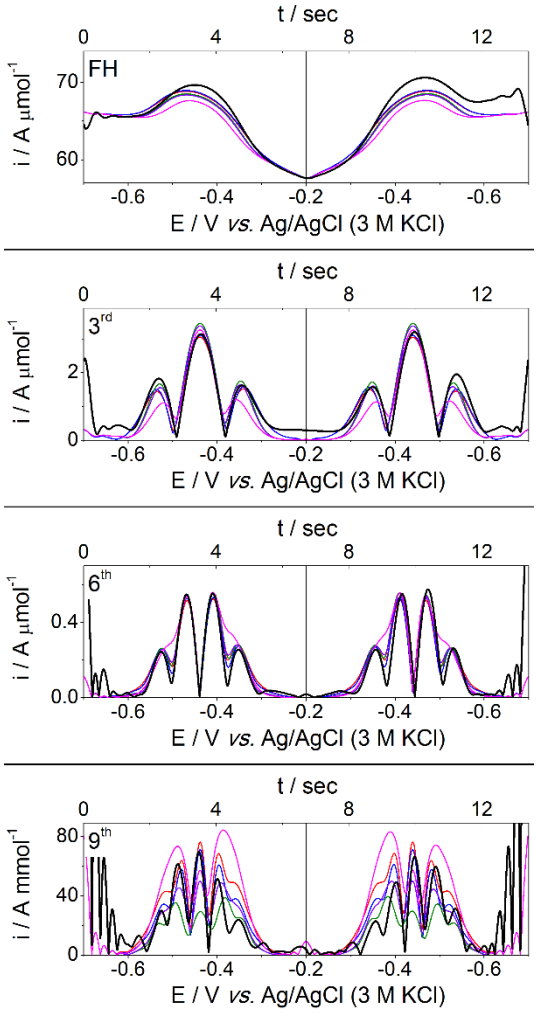

Figure 3. Comparison of fundamental, 3rd, 6th and 9th harmonic components of experimental FTAC voltammogram obtained with a GlcOx-modified MWCNT-rGO electrode in contact with 0.5 M K_2HPO_4 + KH_2PO_4 (pH = 7.0) using f = 9 Hz, ΔE = 0.12 V, v = 0.075 V s^{-1} (*black*) and voltammograms simulated with models given in Table 1: *red* – **I**, $k^0_{0/\cdot-} = k^0_{\cdot-/2-} = 150$ s^{-1}; *blue* - **II**, $k^0_{0/\cdot-} = k^0_{\cdot-/2-} = 190$ s^{-1}; *green* – **III**, $k^0_{0/\cdot-} = k^0_{\cdot-/2-} = 3000$ s^{-1}; *magenta* – as for **III** but using Marcus theory with λ = 0.2 eV, $k^0_{0/\cdot-} = k^0_{\cdot-/2-} = 3900$ s^{-1}; *purple* – **IV**, $k^0_{2e} = 30$ s^{-1}. Other simulation parameters: Γ = 1.5 pmol cm^{-2}, A = 3.46 cm^2, R_u = 71 Ω, nonlinear $C_{DL}(E)$, T = 310 K. Currents are normalized to the amount (mol) of electrochemically active FAD.

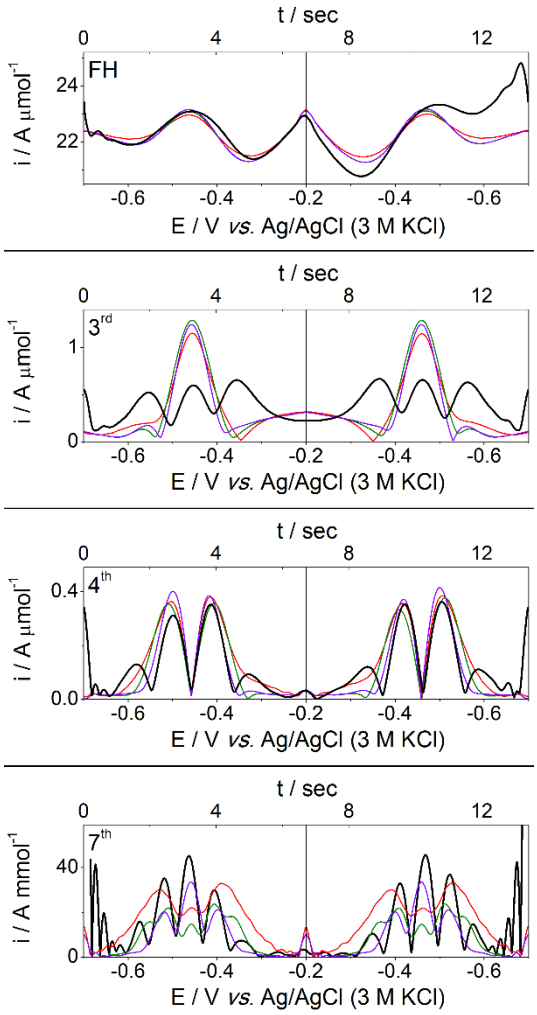

Figure 4. Comparison of fundamental, 3rd, 4th and 7th harmonic components of FTAC voltammograms obtained for a GlcOx-modified SWCNT electrode in contact with 0.5 M K_2HPO_4 + KH_2PO_4 (pH = 7.0) using f = 9 Hz, ΔE = 0.12 V and v = 0.075 V s^{-1} (*black*) and of simulated voltammograms considering different models (Table 1): *red* – I, $k^0_{0/\cdot-} = k^0_{\cdot-/2-} = 13$ s^{-1}; *green* – III, $k^0_{0/\cdot-} = k^0_{\cdot-/2-} = 400$ s^{-1}; *purple* – IV, $k^0_{2e} = 5$ s^{-1}. Other simulation parameters: Γ = 0.6 pmol cm^{-2}, A = 4.38 cm^2, R_u = 18 Ω, nonlinear $C_{DL}(E)$, T = 310 K. Currents are normalized to the amount (mol) of electrochemically active FAD.

The comparatively high background current and low surface concentration of the redox active component leads to fundamental harmonic components of the FTAC voltammograms that are dominated by double layer (pseudo)capacitance (C_{DL}) current, which exhibits a complicated dependence on the potential. As a consequence of the non-linearity of $C_{DL}(E)$, background current is also observed in the 2nd and 3rd harmonic components (Figs. 3 and 4). Importantly, the more kinetically sensitive 4th and higher order harmonic components are virtually devoid of the undesired background signals and are dominated by the faradaic response from the FAD cofactor.

Qualitative resemblance of the patterns of the experimental higher order FTACV harmonic data exemplified in Figs. 3 and 4 with those predicted by theory for chemically reversible and electrochemically quasi-reversible surface-confined electron transfer[4] suggests that the electrochemistry of surface confined FAD may be reasonably well described by simplified net reaction 1, or, alternatively, by reactions 2 and 3 with $k^0_{0/\bullet-}$ and $k^0_{\bullet-/2-}$ of the same order of magnitude. Significant differences in $k^0_{0/\bullet-}$ and $k^0_{\bullet-/2-}$ in simulations predict asymmetry and smearing out of maxima and minima features in the higher harmonic patterns. Introduction of this feature might improve agreement between experiment and theory in some cases (Fig. S4a). However, the effect produced by variation of the $k^0_{0/\bullet-}/k^0_{\bullet-/2-}$ ratio is strongly dependent on the relationship between $E^0_{0/\bullet-}$ and $E^0_{\bullet-/2-}$ (*cf.* panels (a) and (b) in Fig. S4, Supporting Information). On this basis, simulations discussed below using reactions 2 and 3 are produced with the assumption of equality of $k^0_{0/\bullet-}$ and $k^0_{\bullet-/2-}$, although if this represents a unique solution is not established unequivocally.

The low-frequency FTAC voltammograms obtained from the GlcOx-modified MWCNT-rGO electrodes have been fitted to all harmonics by simulations based on a range of models (Fig. 3, Table 1) using the Γ values extracted from the charge derived from DC voltammetric data.

Satisfactory agreement between FTACV experiments and theory was not possible for this or any other electrode examined when the $FAD^{0/\bullet-/2+}$ process was assumed to proceed as in reaction 1 *via* a surface-confined simultaneous two-electron transfer with the electrode kinetics described by the BV relationship. Thus, with use of this model, matching the current magnitude of each experimental harmonic component requires use of a different value of the k^0_{2e} parameter, *e.g.* 50 and 5 s^{-1} for fundamental and 6th harmonics, respectively. This is clearly unacceptable. Most significantly, poor agreement in the shapes of experimental and simulated harmonic components is encountered. Thus, inability to use the BV model with reaction 1 to describe the experimentally observed behaviour confirmed the inapplicability of the classical simultaneous two-electron transfer theory[10] for quantification of the FAD electrode kinetics.

Other simulation models for GlcOx-modified MWCNT-rGO in Fig. 3 are based on a mechanism comprising reactions 2 and 3 with E^0 values being equal or differing by 0.4 V and with either BV formalism with α fixed at 0.50 or Marcus theory used to describe the kinetics of the electron transfer and also use of reaction 1 with electrode kinetics now described by Marcus rather than by BV theory. As shown above, ΔE^0 of 0.4 V leads to apparent transformation of reactions 2 and 3 into the simultaneous two-electron transfer and is employed in simulations as an extreme case of the mechanism based on consecutive one-electron transfers.

Essentially the poorest agreement between theory and experimental data for the GlcOx-modified MWCNT-rGO (see Fig. 3) and rGO composites in terms of fitting both the current magnitude and shape of all detected harmonic components (1st to 10th) was achieved when using reactions 2 and 3 with $E^0_{0/\bullet-}$ and $E^0_{\bullet-/2-}$ differing by 0.4 V and Marcus theory (*magenta* curves in Fig. 3). Other models could be used to produce significantly more acceptable fits of the experimental data in harmonic components below the 7th, but notable differences invariably emerged in the 8th to 10th

harmonics where kinetic (frequency) dispersion is expected to be dominant (Fig. 3). Heuristic comparison of the higher harmonic data obtained with f = 9 Hz leads to the conclusion that the best fit of a mechanism for redox transformation in the FAD cofactor within the GlcOx-modified MWCNT-rGO and rGO composite electrode sets is provided by Marcus electron transfer theory applied to a model based on reactions 2 and 3 with equal E^0 and k^0 values and λ = 0.2 eV, which is at the lower level of realistic values.[30]

Achievement of as good a match of the harmonic components of the FTAC voltammograms obtained for SWCNT-containing electrodes with simulations *via* heuristic procedures were generally less successful because different parameters had to be used to mimic current magnitudes and harmonic patterns (Fig. 4). For example, when the mechanism based on reactions 2 and 3 with BV electrode kinetics was considered, simulations that match the experimental shapes of higher harmonic components (Fig. 4) required $k^0_{0/\bullet-}$ and $k^0_{\bullet-/2-}$ parameters exceeding *ca.* 100 s^{-1} at f = 9 Hz. In contrast, matching the experimentally observed current magnitudes of these well-defined harmonic components required significantly lower $k^0_{0/\bullet-}$ and $k^0_{\bullet-/2-}$ values when using Γ values estimated from the DC voltammetry (Table 1). The discrepancy cannot be explained by errors in determination of Γ, since altering this parameter by a factor of 2 still does not allow an adequate fit of both the experimental current magnitudes and shapes of FTAC voltammograms obtained with SWCNT-based electrodes.

FTAC voltammetry at low frequency: comparison of experimental and simulated data using *e*-science tools. A purely heuristic approach to comparison of theory and experiment as undertaken above is of limited value for a complex mechanism as applies to the redox behaviour of FAD. To quantitatively establish the degree to which different models mimic the experimental FTACV data, the Nimrod/G generic *e*-science tool kit for comparing experimental and modelled

data[25,26] was employed. Nimrod/G performs a sweep of the parameters sought and determines the level of agreement between the experiment and simulation for all possible parameter combinations using the model provided. In this study, the relative difference of the absolute values (ψ) (see Experimental section) was used as a measure of the quality of fit to find the combinations of k^0 and λ parameters, assumed equal in reactions 2 and 3, that provide the best agreement between experimental data obtained for the GlcOx-modified MWCNT-rGO composite with simulations based on Marcus theory. The results are presented in the form of a contour map of ψ plotted versus k^0 and λ, where the lowest value of ψ provides a measure of the best fit. Thus, Nimrod/G analysis provides a quantitative means of ascertainment of the best fit of the model selected to describe the redox chemistry of surface-confined FAD to experimental data.

For the mechanism based on reactions 2 and 3 with $E^0_{0/\bullet-}$ and $E^0_{\bullet-/2-}$ separated by 0.4 V (Fig. 3, *magenta* curves) and regarded as unsuitable in above discussion, Nimrod/G sweep analysis predicts a minimal value of ψ with λ values greater than 100 eV (Fig. S5, Supporting Information). Under these circumstances, the most likely values of $k^0_{0/\bullet-}$ and $k^0_{\bullet-/2-}$ predicted by Nimrod/G with $\lambda > 100$ eV are about 3000 s^{-1} as also deduced from the heuristic approach with simulations based on the BV relationship (Fig. 3). In other words, the best but still poor agreement for the discredited mechanism with $\Delta E^0 = 0.4$ V is achieved when the model is effectively transformed into case **III** in Table 1 (*green* curves in Fig. 3) based on the BV relationship. *E*-science assisted analysis of models based on reactions 2 and 3 with equal $E^0_{0/\bullet-}$ and $E^0_{\bullet-/2-}$ values or use of reaction 1 (cases **II** and **IV** in Table 1, respectively) and seen to be more probable were found by use of the Nimrod/G tool kit to require λ less than 0.3 eV for the best agreement with experiment (Fig. 5).

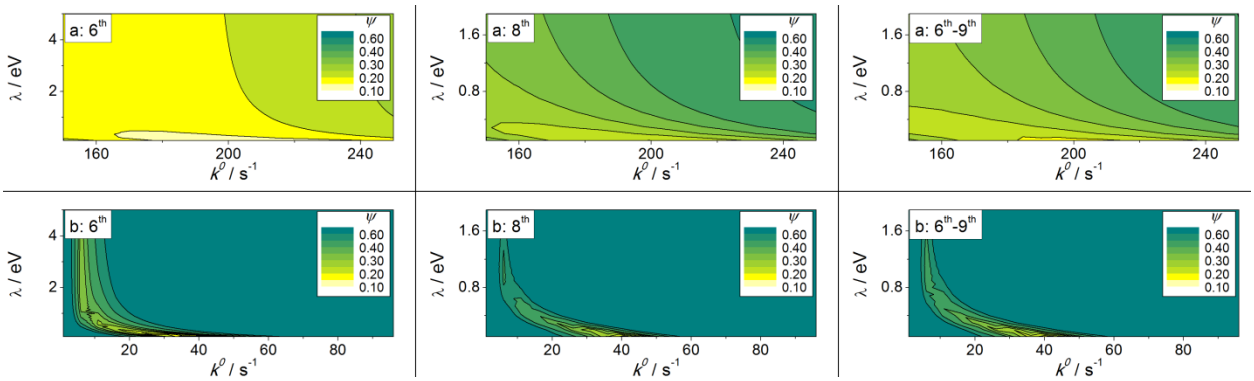

Figure 5. Contour maps showing the relative differences (ψ) between AC harmonic components of the experimental FTAC voltammograms obtained for the GlcOx-modified MWCNT-rGO electrode using f = 9 Hz, ΔE = 0.12 V and v = 0.075 V s^{-1} (original data shown in part in Fig. 3) and simulated voltammograms for (a) reactions 2 and 3 ($E^0_{0/\bullet-}$ = $E^0_{\bullet-/2-}$ = -0.439 V) and (b) reaction 1 using Marcus theory with λ varied in 0.2 – 5 eV range and (a) $k^0_{0/\bullet-}$ = $k^0_{\bullet-/2-}$ varied from 150 to 250 s^{-1} or (b) k^0_{2e} varied from 1 to 96 s^{-1}. Other simulation parameters as in Fig. 3. Individual contour maps obtained for the 6th and 8th harmonic components and aggregate contour maps for the 6th, 7th, 8th and 9th harmonic components are presented.

The minimum ψ values (ψ_{min}) found on the '$k^0 - \lambda$' surface ($\lambda \geq 0.2$ eV) turned out to be harmonic component dependent. For the mechanism based on reactions 2 and 3 with ΔE^0 = 0.4 V, ψ_{min} of 0.18 was found for harmonics 4 to 6, while ψ_{min} of 0.35 and higher was encountered in the 8th and 9th harmonic components. Similar harmonic dependent ψ_{min} values were found for the model based on the instantaneous two-electron transfer (Fig. 5b). The lowest values of ψ_{min} and, most importantly, the most uniform harmonic distribution of ψ_{min} was found when the mechanism based on reactions 2 and 3 with ΔE^0 = 0.0 V was employed in simulations (Fig. 5a). Although the level

of disagreement between the experiment and theory calculated as an aggregate ψ for 6th, 7th, 8th and 9th harmonic components is still substantial (ψ_{min} = 0.21), model **II** (Table 1) on this basis is the most adequate, among tested ones, to describe the redox transformation of the surface-confined FAD.

The assumption of equality of $E^0_{0/\bullet-}$ and $E^0_{\bullet-/2-}$ used in model **II** (Table 1) was explored by additional Nimrod/G analysis, when ψ was evaluated as a function of ΔE^0. Each ΔE^0 requires an individual combination of λ and k^0 for reactions 2 and 3 to achieve the best fit of experimental data with simulation. Therefore, the multidimensional $\psi(\Delta E^0; \lambda; k^0)$ dependence was derived with ΔE^0, λ and k^0 parameters varied within the 0.0 - 0.4 V, 0.2 - 13 eV and 200 - 4000 s^{-1} ranges, respectively. For the given experimental FTACV data set examined (GlcOx-modified MWCNT-rGO composite, f = 9 Hz), the $\psi_{min}(\Delta E^0; \lambda; k^0)$ value was found with ΔE^0 = 0.0 V, λ = 0.2 eV and k^0 = 200 s^{-1}, consistent with the data in Table 1 and Fig. 5a.

FTAC voltammetry at high frequency (f = 89 Hz). Although an acceptable quality of agreement between low-frequency FTACV experimental data and simulations was achieved, new valuable information was gained when undertaking analysis of FTAC voltammetric data at a higher frequency of 89 Hz (Fig. 6). As exemplified in Fig. 6d for the GlcOx-modified MWCNT-rGO electrode, use of kinetic parameters deduced on the basis of simulations at 9 Hz do not allow FTAC voltammograms to be well mimicked at 89 Hz. Matching the current magnitudes of the higher order harmonic components obtained at the higher frequency typically required k^0 values *ca.* 3 times higher than used to simulate lower frequency data when using the parameters and models listed in Table 1. Fitting of the shapes of the higher harmonic components experimentally observed at 89 Hz could be achieved with use of k^0 values that exceed those listed in Table 1 by at

least an order of magnitude, but produce simulated curves with current magnitudes that drastically exceed those found in the experimental data for all types of electrodes (Fig. 6).

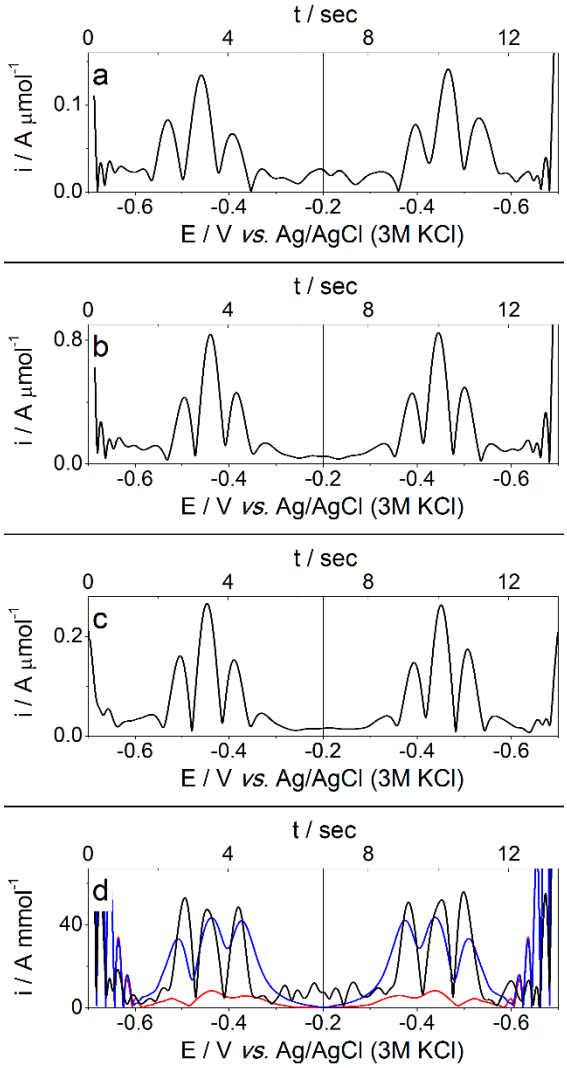

Figure 6. Fifth harmonic components of FTAC voltammograms obtained with GlcOx-modified (a) SWCNT, (b) rGO, (c) SWCNT-rGO and (d) MWCNT-rGO electrodes in contact with 0.5 M K_2HPO_4 + KH_2PO_4 (pH = 7.0) using f = 89 Hz, ΔE = 0.12 V and v = 0.075 V s^{-1}. Panel (d) also contains 5th harmonic components of simulation based on reactions 2 and 3 with Marcus theory (all λ = 0.2 eV) with $k^0_{0/-} = k^0_{-/2-}$ = 190 s^{-1} (*red*) or $k^0_{0/-} = k^0_{-/2-}$ = 450 s^{-1} (*blue*),

$E^0_{0/\bullet-} = E^0_{\bullet-/2-}$ = -0.442 V and other parameters similar to those in Fig. 3. Currents are normalized to the amount (mol) of electrochemically active FAD.

Theory *vs.* experiment discordance. The harmonic and frequency inconsistency of even the best models may be explained by a synergy of at least two effects.

First, electrode heterogeneity of the immobilized FAD structures on the surface of the carbon supports can transform into substantial thermodynamic and kinetic dispersion. Data in Figs. 3, 4 and 6 suggest that the differences in $E^0_{0/\bullet-}$, $E^0_{\bullet-/2-}$ parameters for individual FAD structures may not be too great. In contrast, dispersion in the heterogeneous electron-transfer rate constants could generate $k^0_{0/\bullet-}$, $k^0_{\bullet-/2-}$ values that differ markedly. In the FTACV method, FAD species with very "fast" kinetics would be expected to dominate AC responses in the higher harmonics, particularly at higher frequency (89 Hz) (Fig. 6), while both "faster" and "slower" electron transfers contribute more significantly to the low-frequency FTAC voltammograms (9 Hz). It is highly probable that FAD on the electrode exists in a form attached to GlcOx, as well as in a dissociated form. Thus, two closely related processes may occur simultaneously and contribute to the heterogeneity observed.

Another source of discrepancy between experiment and theory may be a result of a failure to explicitly model gating *viz.* control of the apparent kinetics of the electron transfer associated with the $FAD^{0/\bullet-/2-}$ processes by a coupled chemical or conformational transformation. Indeed, FAD is believed to transform from the "butterfly" conformation to a planar structure upon oxidation (Scheme 1).[9,12,31] Although a conformational change is shown to precede the charge transfer in Scheme 1, it is noted that the true mechanism associated with overall process is unknown. Consequently, a two-electron version of gating is used in Scheme 1 for the sake of simplicity.

As demonstrated by Armstrong *et al.*[29,30] implementation of gating in simulations in surface-confined protein voltammetry can produce a model akin to application of Marcus theory with a very low λ value. Indeed, low reorganization energies in the simulations of the data derived from the GlcOx-modified electrodes provides the best agreement between theoretical predictions and experimental observations. Moreover, the fact that k^0_{app} values required for fitting the higher frequency (89 Hz) FTACV data substantially exceed those derived from analysis of the low-frequency experiments is consistent with gating. That is the conformational change can be outrun at high frequency, so that its influence is more important at low frequency. These and other[9,12,31] observations favour a contribution from conformational changes in the apparent k^0_{app} values for surface-confined FAD.

Scheme 1. Conformational change proposed to accompany electron transfer in FAD.

Effect of carbon support on the efficiency of electron transfer between GlcOx and electrode. Notwithstanding the complexity of modelling the voltammetry for surface-confined FAD, the apparent k^0 values listed in Table 1 may still be used for a semiquantitative comparison of the relative efficiency of the carbon supports in providing electron transfer. On this basis, the presence of SWCNTs in the composites introduces additional heterogeneity and decreases k^0_{app}, even though the highest efficiency of immobilization of FAD was attained with the SWCNT-rGO

samples (Table 1). The largest k^0_{app} values were found with the rGO-MWCNT composites. GlcOx-modified rGO electrodes, free of carbon nanotubes, exhibited both slightly lower efficiencies of immobilization and k^0_{app} values as compared to rGO-MWCNT.

The differences in k^0_{app} values (Table 1) might be partly attributed to differences in conductivity of composite carbon supports. The conductivity of SWCNTs is determined by the relationship between metallic and semiconducting structures[32] and is generally lower than that of MWCNTs which possess higher intrinsic electrical conductivity and usually much greater total number of conductive channels.[33] The rGO materials produced by reduction of GO under conditions employed in this work have been shown to exhibit high electrical conductivity.[34] Thus, conductivity considerations correlate with k^0_{app} values extracted by analysis of the FTACV data (Table 1). This hypothesis also is supported by electrochemical impedance spectroscopy data obtained at -0.70 V (no faradaic current associated with FAD is present), which shows a higher resistance for the SWCNT electrodes relative to rGO and rGO-MWCNT composites.

It is also interesting to note that introduction of 9 wt.% of SWCNT in an rGO support drastically decreases the k^0_{app} value for immobilized FAD (Table 1). Plausibly, incorporation of small amounts of SWCNT compromises the electrical conductivity of the composite electrode. An opposite but smaller effect is observed when rGO is modified by addition of 9 wt. % of MWCNT.

CONCLUSIONS

The FTAC voltammetric technique has been used in conjunction with simulations and data analysis using a heuristic approach as well as *e*-science tools to estimate electrode kinetics parameters associated with the $FAD^{0/\bullet-/2-}$ processes derived from the GlcOx-modified carbon supports. Mechanisms using electron transfer models based on Butler-Volmer or Marcus theory

have been used in simulations of experimental data. Data analysis is complicated by substantial electrode heterogeneity, and hence electrode kinetics dispersion, but it has been shown that the simplest models based on a two-electron simultaneous charge transfer do not adequately describe the kinetics of the redox transformation of the FAD cofactor. With the aid of the Nimrod/G *e*-science tool kit, allowing quantitative estimation of theory-experiment agreement to be performed, Marcus theory with very low reorganization energy ($\lambda \leq 0.3$ eV) is shown to provide the best model for simulation of the experimental FTACV data. Apparent success of this model and comparison of the FTACV data obtained at different frequencies suggest that the electron transfer is gated by conformational changes of the cofactor.[9,12,29-31]

Notwithstanding the imperfections of the models and mechanisms employed in the simulations, k^0_{app} values obtained by FTAC voltammetric analysis allow comparisons to be made of the efficiencies of the electron transfer between the electrode and the FAD cofactor immobilized thereon. Via this approach, it is concluded that utilization of SWCNTs deteriorates the electrode kinetics, while rGO-MWCNT composites provide a more favourable environment for fast communication between FAD and the support.

This study emphasizes the fact that classical theory for quantification of the kinetics of surface-confined electron transfer[10] is not applicable to the overall two-electron FAD-based systems.

ASSOCIATED CONTENT

Supporting Information. Table S1 reporting the surface areas of carbon materials and fabricated electrodes. Fig. S1 demonstrating the band filtering employed in the FT/iFT procedure. Fig. S2 showing optical images of aqueous carbon dispersions. Fig. S3 showing SEM images of drop cast MWCNT and SWCNT layers. Fig. S4 showing the effect of non-equivalence of k^0 values

of the $FAD^{0/\bullet-}$ and $FAD^{\bullet-/2-}$ processes on patterns of simulated AC harmonic components. Fig. S5 showing $\psi/k^0_{0/\bullet-}$, $k^0_{\bullet-/2-}/\lambda_{0/\bullet-}$, $\lambda_{\bullet-/2-}$ contour maps derived from comparison of experimental FTACV data obtained for the GlcOx-modified MWCNT-rGO electrode and voltammograms simulated for the $FAD^{0/\bullet-}$ and $FAD^{\bullet-/2-}$ processes with $E^0_{0/\bullet-}$ = -0.639 V and $E^0_{\bullet-/2-}$ = -0.239 V. This material is available free of charge *via* the Internet at http://pubs.acs.org.

AUTHOR INFORMATION

***Corresponding Authors**

smoulton@uow.edu.au (S.E.M.), Alan.Bond@monash.edu (A.M.B.)

ACKNOWLEDGMENT

Financial support from the Australian Research Council under Discovery Project No. 120101470 is gratefully acknowledged.

REFERENCES

(1) Armstrong, F. A. Recent Developments in Dynamic Electrochemical Studies of Adsorbed Enzymes and Their Active Sites. *Curr. Opin. Chem. Biol.* **2005**, *9*, 110-117.

(2) Leger, C.; Bertrand, P. Direct Electrochemistry of Redox Enzymes as a Tool for Mechanistic Studies. *Chem. Rev.* **2008**, *108*, 2379–2438.

(3) Bond, A. M.; Duffy, N. W.; Guo, S.-X.; Zhang, J.; Elton, D. Changing the Look of Voltammetry. Can FT Revolutionize Voltammetric Techniques as It Did for NMR? *Anal. Chem.* **2005**, *77*, 186A-195A.

(4) Stevenson, G. P.; Lee, C.-Y.; Kennedy, G. F.; Parkin, A.; Baker, R. E.; Gillow, K.; Armstrong, F. A.; Gavaghan, D. J.; Bond, A. M. Theoretical Analysis of the Two-Electron Transfer Reaction and Experimental Studies with Surface-Confined Cytochrome *c* Peroxidase Using Large-Amplitude Fourier Transformed AC Voltammetry. *Langmuir* **2012**, *28*, 9864-9877 and references therein.

(5) Zhou, M.; Wang, J. Biofuel Cells for Self-Powered Electrochemical Biosensing and Logic Biosensing: A Review. *Electroanal.* **2012**, *24*, 197-209.

(6) Ansari, S. A.; Husain, Q. Potential Applications of Enzymes Immobilized on/in Nano Materials: A Review. *Biotech. Adv.* **2012**, *30*, 512-523.

(7) Chen, C.; Xie, Q.; Yang, D.; Xiao, H.; Fu, Y.; Tan, Y.; Yao, S. Recent Advances in Electrochemical Glucose Biosensors: A Review. *RSC Adv.* **2013**, *3*, 4473-4491.

(8) Willner, I.; Yan, Y.-M.; Willner, B.; Tel-Vered, R. Integrated Enzyme-Based Biofuel Cells – A Review. *Fuel Cells* **2009**, *9*, 7-24.

(9) Goran, J. B.; Mantilla, S. M.; Stevenson, K. J. Influence of Surface Adsorption on the Interfacial Electron Transfer of Flavin Adenine Dinucleotide and Glucose Oxidase at Carbon Nanotube and Nitrogen-Doped Carbon Nanotube Electrodes. *Anal. Chem.* **2013**, *85*, 1571-1581.

(10) Laviron, E. General Expression of the Linear Potential Sweep Voltammogram in the Case of Diffusionless Electrochemical Systems. *J. Electroanal. Chem* **1979**, *101*, 19-28.

(11) Bard, A. J.; Faulkner, L. R. *Electrochemical Methods: Fundamentals and Applications.* 2nd Edition; John Wiley & Sons, Inc.: New York, USA, 2001.

(12) Birss, V. I.; Elzanowska, H.; Turner, R. A. The Electrochemical Behavior of Flavin Adenine Dinucleotide in Neutral Solutions. *Can. J. Chem.* **1988**, *66*, 86–96.

(13) Smith, E. T.; Davis, C. A.; Barber, M. J. Voltammetric Simulations of Multiple Electron Transfer/Proton Transfer Coupled Reactions: Flavin Adenine Dinucleotide as a Model System. *Anal. Biochem.* **2003**, *323*, 114-121.

(14) Cable, M.; Smith, E. T. Identifying the n = 2 Reaction Mechanism of FAD through Voltammetric Simulations. *Anal. Chim. Acta* **2005**, *537*, 299-306.

(15) Grosse, W.; Champavert, J.; Gambhir, S.; Wallace, G. G.; Moulton, S. E. Aqueous Dispersions of Reduced Graphene Oxide and Multi Wall Carbon Nanotubes for Enhanced Glucose Oxidase Bioelectrode performance. *Carbon* **2013**, *61*, 467-475.

(16) Wang, Y.; Yao, Y. Direct Electron Transfer of Glucose Oxidase Promoted by Carbon Nanotubes is Without Value in Certain Mediator-Free Applications. *Microchim. Acta* **2012**, *176*, 271-277.

(17) Hummers, W. S.; Offeman, R. E. Preparation of Graphitic Oxide. *J. Amer. Chem. Soc.* **1958**, *80*, 1339–1339.

(18) Kovtyukhova, N. I.; Ollivier, P. J.; Martin, B. R.; Mallouk, T. E.; Chizhik, S. A.; Buzaneva, E. V.; Gorchinskiy, A. D. Layer-by-Layer Assembly of Ultrathin Composite Films from Micron-Sized Graphite Oxide Sheets and Polycations. *Chem. Mater.* **1999**, *11*, 771-778.

(19) Gao, F.; Courjean, O.; Mano, N. An Improved Glucose/O_2 Membrane-Less Biofuel Cell through Glucose Oxidase Purification. *Biosensors and Bioelectronics*, **2009**, *25*, 356-361.

(20) Bateman R. C.; Evans, J. A. Using the Glucose Oxidase/Peroxidase System in Enzyme Kinetics. *J. Chem. Educ.* **1995**, *72*, 240-241.

(21) Zhu, Y.; Murali, S.; Cai, W.; Li, X.; Suk, J. W.; Potts, J. R.; Ruoff. R. S. Graphene and Graphene Oxide: Synthesis, Properties, and Applications. *Adv. Mater.* **2010**, *22*, 3906–3924.

(22) Feldberg, S. W. Implications of Marcus-Hush Theory for Steady-State Heterogeneous Electron Transfer at an Inlaid Disk Electrode. *Anal. Chem.* **2010**, *82*, 5176-5183 and references therein.

(23) http://www.garethkennedy.net/MECSim.html.

(24) Mashkina, E.; Bond, A. M. Implementation of a Statistically Supported Heuristic Approach to Alternating Current Voltammetric Harmonic Component Analysis: Re-evaluation of the Macrodisk Glassy Carbon Electrode Kinetics for Oxidation of Ferrocene in Acetonitrile. *Anal. Chem.* **2011**, *83*, 1791-1799.

(25) http://messagelab.monash.edu.au.

(26) Mashkina, E.; Peachey, T.; Lee, C.-Y.; Bond, A. M.; Kennedy, G. F.; Enticott, C.; Abramson, D.; Elton, D. M. Estimation of Electrode Kinetic and Uncompensated

Resistance Parameters and Insights into Their Significance Using Fourier Transformed ac Voltammetry and e-Science Software Tools. *J. Electroanal. Chem*, **2013**, *690*, 104–110.

(27) Cherstiouk, O. V.; Simonov, A. N.; Moseva. N. S.; Cherepanova, S. V.; Simonov. P. A.; Zaikovskii, V. I.; Savinova, E. R. Microstructure Effects on the Electrochemical Corrosion of Carbon Materials and Carbon-Supported Pt Catalysts. *Electrochim. Acta* **2010**, *55*, 8453–8460 and references therein.

(28) Wilson, R.; Turner, A. P. F. Glucose Oxidase: An Ideal Enzyme. *Biosensors and Bioelectronics* **1992**, *7*, 165-185.

(29) Jeuken, L. J. C.; Jones, A. K.; Chapman, S. K.; Cecchini, G.; Armstrong, F. A. Electron-Transfer Mechanisms through Biological Redox Chains in Multicenter Enzymes. *J. Am. Chem. Soc.* **2002**, *124*, 5702-5713.

(30) Hirst, J.; Armstrong, F. A. Fast-Scan Cyclic Voltammetry of Protein Films on Pyrolytic Graphite Edge Electrodes: Characteristics of Electron Exchange. *Anal. Chem.* **1998**, *70*, 5062-5071.

(31) Hemmerich, P.; Veeger, C.; Wood, H. C. S. Progress in the Chemistry and Molecular Biology of Flavins and Flavocoenzyme. *Angew. Chem. Int. Ed.* **1965**, *4*, 671-687.

(32) Chen, Y.; Ng, A. K.; Bai, S.; Si, R.; Wei, L.; Wang, Q. In *Carbon Nanotubes and Their Applications*; Zhang, Q., Ed.; Carbon-Based Nanomaterials; Pan Stanford Publishing Pte. Ltd.: Singapore, 2012; Vol. 1, pp. 121-148.

(33) Bao, W. S.; Meguid, S. A.; Zhu, Z. H.; Meguid, M. J. Modeling Electrical Conductivities of Nanocomposites with Aligned Carbon Nanotubes. *Nanotechnology* **2011**, *22*, 485704 (8pp).

(34) Shin, H.-J.; Kim, K. K.; Benayad, A.; Yoon, S.-M.; Park, H. K.; Jung, I.-S.; Jin, M. H.; Jeong, H.-K.; Kim, J. M.; Choi, J.-Y.; Lee, Y. H. Efficient Reduction of Graphite Oxide by Sodium Borohydride and Its Effect on Electrical Conductance. *Adv. Funct. Mater.* **2009**, *19*, 1987–1992.

For TOC only

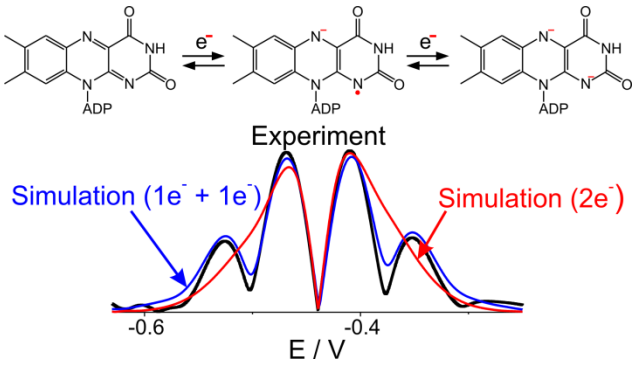
e⁻
e⁻
NH
O
N
ADP
Experiment
Simulation (1e⁻ + 1e⁻)
Simulation (2e⁻)
-0.6
-0.4
E / V